Available online at www.sciencedirect.com
SCIENCE DIRECT®
Tetrahedron: Asymmetry
Tetrahedron: *Asymmetry* 16 (2005) 2993–2997

The bidentate complexes of (*R*,*R*)- and *meso*-α,α′-bis(trifluoromethyl)-9,10-anthracenedimethanol with *cis*-1-amino-2-indanol

Carla Estivill,[a] Marta Pomares,[a] Martin Kotev,[b] Petko Ivanov[a,b] and Albert Virgili[a,*]

[a]*Departament de Química, Universitat Autònoma de Barcelona, Bellaterra, 08193 Barcelona, Spain*
[b]*Institute of Organic Chemistry with Centre of Phytochemistry, Bulgarian Academy of Sciences, ul. Akad. G. Bonchev, Bloc 9, 1113 Sofia, Bulgaria*

Received 25 May 2005; revised 8 July 2005; accepted 8 August 2005

Abstract—The enantiorecognition of 1-aminoindane **3** and *cis*-1-amino-2-indanol **2** by (*R*,*R*)-α,α′-bis(trifluoromethyl)-9,10-anthracenedimethanol **1** is reported. The examination of the bidentate associations between **1** and **2** revealed that the *cisoid* conformation of **1** is responsible for the separation of the NMR signals. Two types of bimodal associations resulted from a *cisoid* conformation when *meso*-**1** isomer was tested. Molecular mechanics modelling studies gave the possible structures of the associate species.

1. Introduction

The composition of a mixture of enantiomers can be determined by NMR when chiral solvating agents (CSA) are used.[1] The enantiomers of α,α′-bis(trifluoromethyl)-9,10-anthracenedimethanol[2] **1** (Fig. 1) were found to present very high CSA activity through the formation of association complexes with enantiomeric substrates that show different complexation properties, thus inducing different magnetic responses in NMR spectroscopy.

The presence of $CHOHCF_3$ stereogenic group affords the necessary points for intermolecular association 'blended' by the chiral character. At the same time, the anthracene ring, in addition to enhancing π-stacking interactions with other π-systems, induces magnetic anisotropy to closely positioned groups and atoms that will vary depending mainly on the geometry of the complex and on the binding constant. Due to the bifunctionality of **1**, the association capacity increases,[3] and when the substrate is also a polyfunctional compound, bidentate associates are possible. In this case, **1** changes its average conformation from the *transoid* to the *cisoid* and produces bidentate complexes, as for example, with benzenedimethanols.[4]

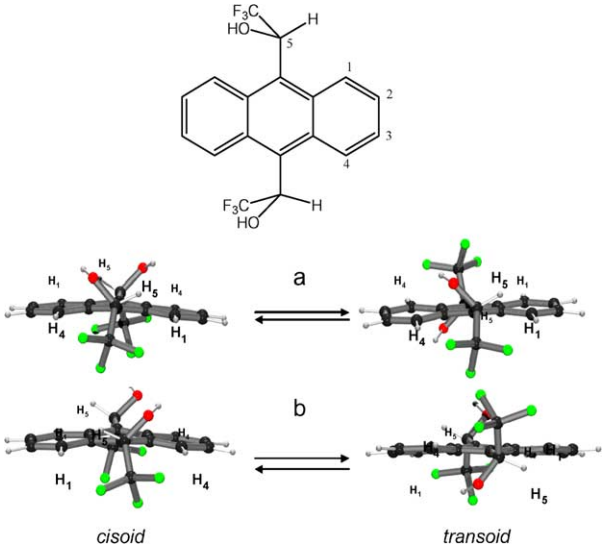

Figure 1. Structure, atomic numbering and conformational equilibrium of (a) (*R*,*R*)-α,α′-bis(trifluoromethyl)-9,10-anthracenedimethanol (*R*,*R*)-1 and (b) *meso*-α,α′-bis(trifluoromethyl)-9,10-anthracenedimethanol *meso*-**1**.

NMR spectroscopy in chiral solvents allows enantiomers to be distinguished, thus providing means for the assignment of their stereochemistry.[5] Chiral oriented phases[6] afford a new way to differentiate chiral

* Corresponding author. E-mail: albert.virgili@uab.es

0957-4166/$ - see front matter © 2005 Elsevier Ltd. All rights reserved.
doi:10.1016/j.tetasy.2005.08.011

molecules. The utilization of chiral solvating agents (CSA) is a very common and powerful technique to assess the composition of mixtures of enantiomers.[7]

cis-1-Amino-2-indanol **2** is a molecule that has useful applications in several fields, with its chiral activity being the crucial characteristic.[8] The ability to determine the chiral composition of a mixture of enantiomers of **2** (by NMR using a CSA) seems to be a very important methodology of practical significance. As **2** is a bifunctional compound, when one of the enantiomers of α,α′-bis(trifluoromethyl)-9,10-anthracenedimethanol **1** is used, then highly ordered diastereomeric bidentate complexes are formed. Herein, we report on the association of the isomers [(*R*,*R*) and *meso*] of **1** with **2** and the structure of bidentate complexes. The high kinetic stability of this type of bidentate associate is also verified. An examination of the association of (*R*,*R*)-**1** with 1-aminoindane **3** confirms its capacity as CSA.

2. Results and discussion

For determining the enantiomers of 1-aminoindane **3**, 3 mg of compound **3** was dissolved in 0.5 mL of $CDCl_3$ and several portions of 0.5 equiv of **1** added. After each addition, ^1H NMR was obtained resulting in an enantiodifferentiation on the protons H_{2S}, H_{2R}, H_{3R} and H_{3S}.

Surprisingly, H_1, which belongs to the stereogenic carbon atom, was not recognized. The experiment was repeated until maximum differentiation was achieved. Figure 2 presents ^1H NMR after the addition of 2 equiv of **1**. The addition of one of the pure enantiomers confirmed that the most shielded protons were those of the (*R*)-**3** enantiomer. The maximum (and a very good) separation of enantiomers was achieved with the addition of only 1.5 equiv of (*R*,*R*)-**1** (Fig. 3).

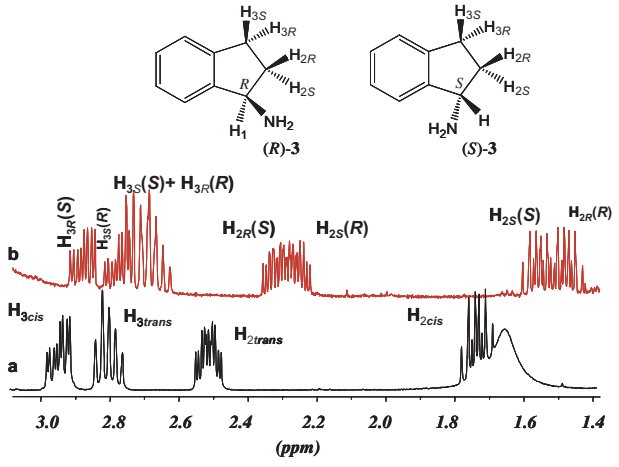

Figure 2. Enantiodifferentiation of 1-aminoindane **3** at 298 K in $CDCl_3$: (a) pure *rac*-**3**. (b) *rac*-**3** after the addition of 2 equiv of (*R*,*R*)-**1**. Protons *cis* and *trans* are numbered with respect to the amino group.

Similar essays were also carried out with *cis*-1-amino-2-indanol **2** but using a mixture (1*R*,2*S*)-**2**/(1*S*,2*R*)-**2** of 3:1. Mean differentiation was observed for H_1 and H_3.

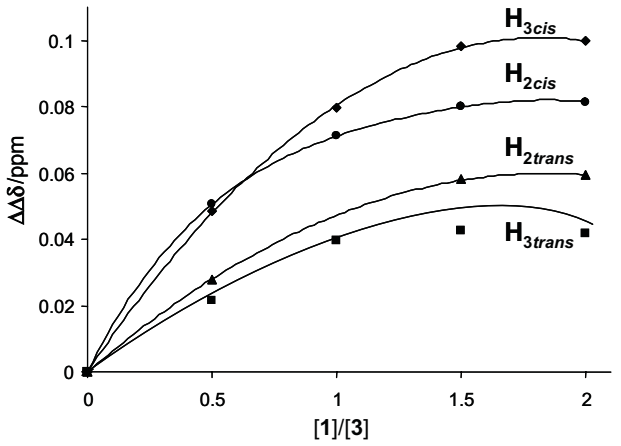

Figure 3. Variation of the difference of chemical shifts ($\Delta\delta S - \Delta\delta R$) for various protons of enantiomers of **3** when several portions of 0.5 equiv of (*R*,*R*)-**1** were added at 298 K.

Protons H_{3cis} and H_{3trans} are more shielded in the (1*S*,2*R*)-**2** enantiomer, while H_1 in (1*R*,2*S*)-**2** is the most shifted to higher fields. Figure 4 shows two parts of the ^1H NMR spectra of the mixture of enantiomers of **2** and the enantiodifferentiation induced by the addition of (*R*,*R*)-**1.**

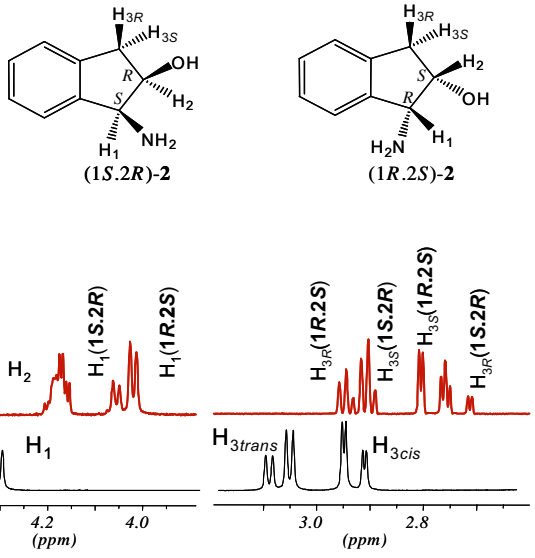

Figure 4. Enantiodifferentiation of a 3:1 mixture of (1*R*,2*S*)/(1*S*,2*R*) *cis*-1-amino-2-indanol **2** (298 K, $CDCl_3$). (a) Without CSA. (b) After the addition of 2 equiv of (*R*,*R*)-**1**. Protons *cis* and *trans* are numbered with respect to the functional groups.

Figure 5 displays the tendency of the enantiodiscrimination for the cited protons of **2** when CSA was added. Again we have to emphasize that maximum and most effective enantiodiscrimination resulted from the addition of only 1 equiv of **1**.

Although **2** is a bifunctional compound, it forms 1:1 complexes with **1** as the Job Plot[9] demonstrated.

The study of the binding constants at two temperatures was carried out using an equimolar method[10] where the

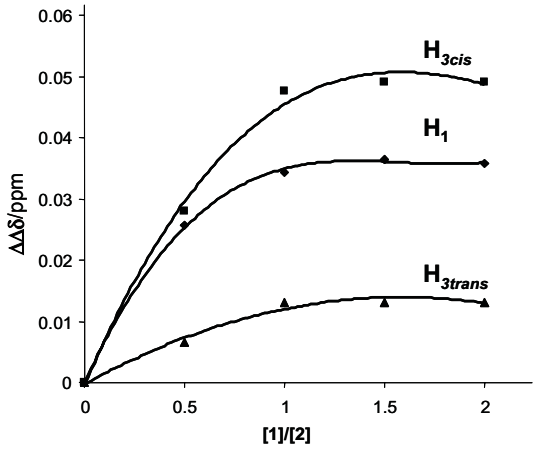

Figure 5. Evolution of the enantiodiscrimination between several protons of the enantiomers of **2** when several portions of 0.5 equiv of (*R*,*R*)-**1** were added.

plotting of the variations of chemical shifts ($\Delta\delta$) of several protons of the substrate versus $(\Delta\delta/S^{o})^{1/2}$ appears as a straight line. The changes of the chemical shifts of H_1, H_{3cis} and H_{3trans} of **2** gave us a mean value for the constant *K*, while for **3**, we used average value from the variation of the chemical shift of H_1, H_{2cis}, H_{2trans}, H_{3cis} and H_{3trans} (Table 1). A higher ordered structure of the bidentate complexes involves an entropic difference between the complexes of **2** and **3** with **1** that could be the factor responsible for the differences shown between their thermodynamic stabilities.

Table 1. Binding constants (and standard deviation) at 268 and 298 K for the association of enantiomers of *cis*-1-amino-2-indanol **2** and 1-aminoindane **3** with (*R*,*R*)-9,10-anthracenedimethanol **1**

Compound	*T* (K)	*K*/*M*	ΔG^{o}/kJ mol^{-1}
(*R*)-**3**	268	88 ± 8	−10.0 ± 0.2
(*S*)-**3**	268	107 ± 14	−10.4 ± 0.3
(*R*)-**3**	298	39 ± 9	−9.1 ± 0.5
(*S*)-**3**	298	96 ± 15	−11.3 ± 0.4
(1*S*,2*R*)-**2**	268	39 ± 7	−8.2 ± 2.2
(1*R*,2*S*)-**2**	268	65 ± 14	−9.3 ± 3.0
(1*S*,2*R*)-**2**	298	19 ± 1	−7.3 ± 0.1
(1*R*,2*S*)-**2**	298	18 ± 3	−7.1 ± 1.5

The straight lines obtained by the equimolar method also allowed us to extrapolate the chemical shifts of the protons of the substrate in a hypothetical isolated complex. The two straight lines obtained at two temperatures converge on a value for each proton. Table 2 shows the values for the association between (*R*,*R*)-**1** and each enantiomer of **2** and **3**.

In order to examine the structure of the complexes by the modification of the NMR signals of **1**, we prepared the individual associations between (*R*,*R*)-**1** and each enantiomer of *cis*-**2** ([**1**]/[**2**] = 1.2). The ^{1}H NMR spectra were recorded at 250 K. The identification of the signals was carried out by using standard NMR sequences of magnetization transfer and NOE transfer.

Figure 6 represents the ^{1}H NMR spectra of the association of (*R*,*R*)-**1** with (1*R*,2*S*)-**2** and with (1*S*,2*R*)-**2**. The signals of H_1 and H_5 of (*R*,*R*)-**1** (basically corresponding to the *cisoid* forms) were modified to higher fields, indicating a preferred bidentate association through this conformation. The equilibrium between the *cisoid* and the *transoid* conformations of (*R*,*R*)-**1** shifted to the *cisoid* one in both cases, changing from a ratio of 1.2 to 2.2 and 1.9, respectively (250 K). The H_4 proton of (*R*,*R*)-**1** was only slightly altered. Each one of these complexes should be retained by the formation of hydrogen bonds between the hydroxyl groups of (*R*,*R*)-**1** and the amino group and/or the hydroxyl group of the *cis*-aminoindanol **2**, the only difference being the chirality of the carbon atoms that support the latter functional groups. Two simultaneous interactions are

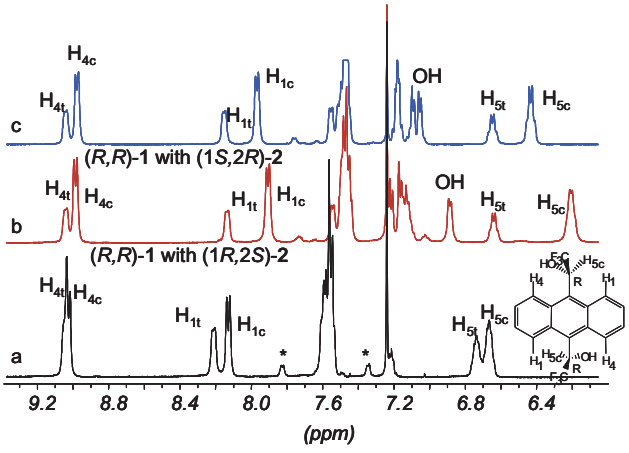

Figure 6. The aromatic parts of the ^{1}H NMR (250 K in $CDCl_3$) spectra of: (a) (*R*,*R*)-**1**, (b) the association of (*R*,*R*)-**1** with (1*R*,2*S*)-**2**, (c) the association of (*R*,*R*)-**1** with (1*S*,2*R*)-**2**. Subscript 'c' corresponds to *cisoid* form and subscript 't' is for *transoid* form. *Anthraquinone degradation impurities.

Table 2. Extrapolated chemical shifts (ppm) of several protons of the complexes resulting from the association of the enantiomers of **3** and *cis*-**2** with the dialcohol (*R*,*R*)-**1** (standard deviation)

Complex	δ_{H_1}	$\delta_{H_{3trans}}$	$\delta_{H_{3cis}}$	$\delta_{H_{2trans}}$	$\delta_{H_{2cis}}$
3 (Pure)	4.344	2.829	2.976	2.525	1.718
(*R*,*R*)-**1**/*R*-**3**	4.019 ± 0.009	2.620 ± 0.008	2.705 ± 0.009	2.145 ± 0.009	1.374 ± 0.011
(*R*,*R*)-**1**/*S*-**3**	4.002 ± 0.006	2.667 ± 0.003	2.845 ± 0.003	2.209 ± 0.006	1.476 ± 0.006
cis-**2** (Pure)	4.362	3.116	2.996	—	—
(*R*,*R*)-**1**/(1*R*,2*S*)-**2**	3.421 ± 0.100	2.634 ± 0.032	2.521 ± 0.090	—	—
(*R*,*R*)-**1**/(1*S*,2*R*)-**2**	3.451 ± 0.043	2.653 ± 0.013	2.420 ± 0.020	—	—

possible in the *cisoid* conformation, producing a longer life-time for the *bidentate* complex and, accordingly, greater observed influence.

The chemical shifts of H_1 and H_5 of (*R*,*R*)-**1**, are larger affected in the association with (1*R*,2*S*)-**2** than with (1*S*,2*R*)-**2** concluding a greater influence of the associated in the observed average in the first complex.

Although the C_2 symmetry of (*R*,*R*)-**1** is lost in the association, only one set of *cisoid* and *transoid* signals for H_1, H_4 and H_5 of **1** was found, confirming the observation of the kinetic average.

Surprisingly, when we analyzed the spectrum from an analogous experiment, but using *meso*-**1**[2] instead of (*R*,*R*)-**1**, we distinguished two modes (α and β) of bidentate interactions between both enantiomers of **2**. These correspond to the two possible relative orientations of the two components, (1*R*,2*S*)-**2** and *cisoid meso*-**1**. We confirmed this result using the other enantioisomer (1*S*,2*R*)-**2**, that gives the corresponding enantiomeric complex and yielding the analogous NMR spectrum.

Here also the equilibrium between the *cisoid* and the *transoid* conformations of *meso*-**1** shifted to the *cisoid* one, changing from a ratio of 1:1 (*transoid*:*cisoid*) to a ratio approximately of 1:1:1 (*transoid*:*cisoid* α:*cisoid* β) (250 K). Moreover, the *transoid* form can be observed slightly separated (H_1 and H_5) in two forms (named also α and β).

Figure 7 shows ^{1}H NMR spectrum for the association of *meso*-**1** with (1*R*,2*S*)-**2** and (1*S*,2*R*)-**2** obtaining the same results. The small increment of the ratio of *meso*-**1** in spectrum (c) justifies the slight decrease of the chemical shift. We observed four different associates: two implying the *transoid* conformation and two more where the *cisoid* form has the leading role. In the latter, the signals of protons H_1, H_4 and H_5 are extraordinarily modified. The identification of each group of signals was made, as before, with NMR experiments (at 250 K) where the exchange was detectable (Fig. 8).

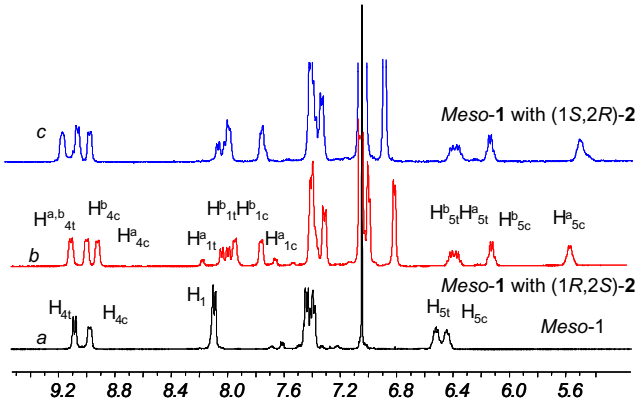

Figure 7. The aromatic part of the ^{1}H NMR spectra (250 K in $CDCl_3$) of associations: (a) *meso*-**1**, (b) *meso*-**1** with (1*R*,2*S*)-**2** (ratio 0.5) and (c) *meso*-**1** with (1*S*,2*R*)-**2** (ratio 0.7).

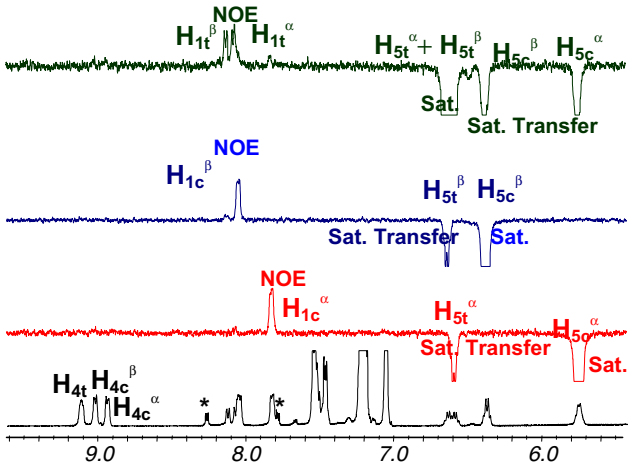

Figure 8. Aromatic part of ^{1}H NMR spectra (250 K in $CDCl_3$). (a) *meso*-**1** (*RS*,*SR*)-**1**. (b), (c) and (d) NOE spectra (obtained using 1D DPFGNOE sequence) after saturation of the indicated signals. *Anthraquinone degradation impurities.

Each *cisoid* form is equilibrated with only one *transoid* form, but no transformation between the two *cisoid* or between the two *transoid* forms is observed (no saturation transfer). As before, the signals of the *cisoid* associates are extensively modified and correspond to the two possible associate species resulting from the two possible modes of approach: (i) the OH from the (*R*)-centre of *meso*-**1** with the amino group of (1*R*,2*S*)-**2** and the OH from the (*S*)-centre of *meso*-**1** with the hydroxyl of (1*R*,2*S*)-**2** and (ii) the OH from the (*R*)-centre of *meso*-**1** with the hydroxyl group of (1*R*,2*S*)-**2** and the OH from the (*S*)-centre of *meso*-**1** with the amino group of (1*R*,2*S*)-**2**. We can say that enantiopure 1,2-*cis*-aminoindanol recognizes the two enantiotopic parts of *meso*-**1** developing two different association complexes. The weak association of the *transoid* conformers of *meso*-**1** allows a slight distinction of two possible ways of complexation, doubling the signals of H_{1t} and H_{5t}.

The structure of *meso*-**1** differs from the corresponding enantiomer (*R*,*R*)-**1** in the relative position of the OH groups. While in the first enantiomer the hydroxyl groups lie on the same side of one anthracene ring face, in (*R*,*R*)-**1** they are located on opposite sides of one anthracene ring face (Fig. 1). In that case, complexation with *meso*-**1** allows a deeper penetration of the aromatic ring of the substrate by the more liberated side. This structural difference can justify the greater magnetic influence between the anisotropic and chiral groups and explain the greater difficulty in destroying the formed complex (longer lifetime of the complex).

The MACROMODEL and BATCHMIN V5.0 software packages were used for the molecular modelling studies,[11] with the AMBER* all-atom force field[12] and the GB/SA (cavity + van der Waals + electrostatic polarization term) solvation model to simulate $CHCl_3$.[13–15] A dielectric constant of 1.0 was used for estimating electrostatic interactions. Extended nonbonded cut-off distances were

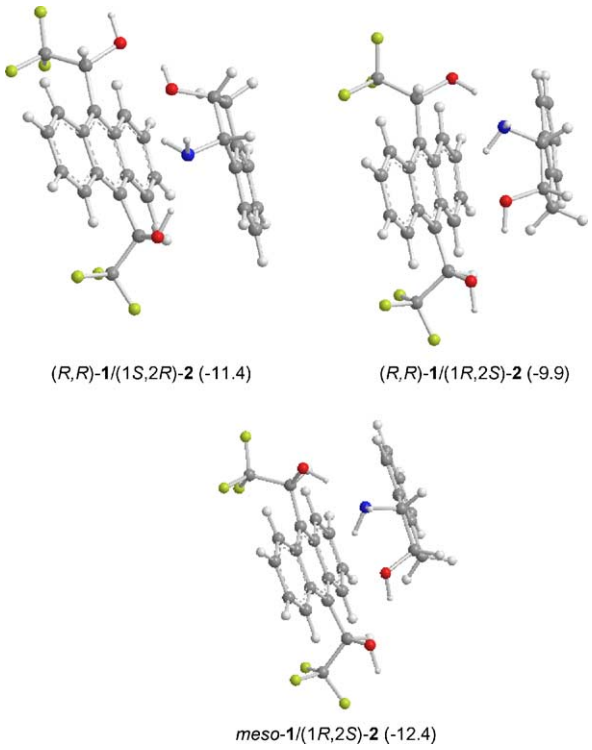

Figure 9. Views of the lowest energy structures for the associations between (*R*,*R*)-**1** with (1*S*,2*R*)-**2** and (1*R*,2*S*)-**2** and *meso*-**1** with (1*R*,2*S*)-**2**. The computed energies of complex formation are given in parentheses (in kcal mol^{-1}).

set to 10.0 Å for the van der Waals and 20.0 Å for the electrostatic interactions.

The geometry optimizations were carried out at two stages: a preliminary minimization with the Polac–Ribie conjugate gradient (CG) method, followed by full-matrix Newton–Raphson minimization.[11] The maximum number of iterations provided was sufficient enough to ensure convergence in all cases. Molecular graphics was used to generate different starting geometries for the complexes: after being placed at the distance 4.5–5.0 Å from **1**, molecule **2** was rotated by 30° steps (from 0° to 360°) with the two functional groups facing the *cisoid* conformation of **1** from the side of the hydroxyl groups. The different possibilities for rotations of the hydroxyl and amino groups were also explored. About 30 starting structures were used in each case. In the same manner, the complexes with the plane of **2** which are perpendicular to the plane of **1** were examined as well as the case when **1** is in the *transoid* conformation.

For each complex, several structures with energies that differ less than 2 kcal/mol were obtained. However, in all cases, the more stable association structures are bidentates complexes with similar pattern (Fig. 9).[16] Similar hydrogen bonds participate in the structures and the parallelism between the aromatic rings is also a common factor.

meso-**1**, according to our computation data, makes stronger complexes than (*R*,*R*)-**1**, as can be also deduced from the most shifted signals of the ^{1}H NMR spectra.

Molecular mechanics studies of the self-associations (1*S*,2*R*)-**2**/(1*S*,2*R*)-**2** yielded energies of complexations ca. 7 kcal mol^{-1}. Thus, self-associations cannot perturb the preferred formation of complexes between **2** and **1**.

Acknowledgements

Financial support from CICYT (Project BQU2003-01231)) is gratefully acknowledged. CIRIT (Generalitat de Catalunya, Catalonia, Spain) and the MECD (Spain) are also acknowledged for Visiting Professor Grant to one of us (P.I.). Minor financial support from NSF, Bulgaria (Project X-1406) is acknowledged.

References

1. Pirkle, W. H. *J. Am. Chem. Soc.* **1966**, *88*, 1837.
2. Pomares, M.; Sánchez-Ferrando, F.; Virgili, A.; Alvarez-Larena, A.; Piniella, J. F. *J. Org. Chem.* **2002**, *67*, 753–758.
3. Ridder, D.; Hwemderlich, H.; Braun, M. *Eur. J. Org. Chem.* **1998**, 1071–1076.
4. Estivill, C.; Ivanov, P. M.; Pomares, M.; Sánchez-Aris, M.; Virgili, A. *Tetrahedron: Asymmetry* **2004**, *15*, 1431–1436.
5. (a) Kobayashi, Y.; Hayashi, N.; Choon-Hong, T.; Kishi, Y. *Org. Lett.* **2001**, *3*, 2245–2248; (b) Hayashi, N.; Kobayashi, Y.; Kishi, Y. *Org. Lett.* **2001**, *3*, 2249–2252; (c) Hayashi, N.; Kobayashi, Y.; Kishi, Y. *Org. Lett.* **2001**, *3*, 2253–2255.
6. (a) Aroulanda, C.; Merlet, D.; Courtieu, J.; Lesot, P. *J. Am. Chem. Soc.* **2001**, *123*, 12059–12066; (b) Lesot, P.; Sarfati, M.; Courtieu, J. *Chem. Eur. J.* **2003**, *9*, 1724–1745.
7. (a) Parker, D. *Chem. Rev.* **1991**, *91*, 1441–1457; (b) Iuliano, A.; Bartalucci, D.; Ucello-Barretta, G.; Balzano, F.; Salvadori, P. *Eur. J. Org. Chem.* **2001**, 2177–2184; (c) Wenzel, T. J.; Wilcox, J. D. *Chirality* **2003**, *15*, 256–270.
8. Senenayake, C. H. *Aldrichimica* **1998**, *31*, 3–15.
9. Job, P. *Ann. Chim.* **1928**, *9*, 113–203.
10. Bouquant, J.; Chuche, J. *Tetrahedron Lett.* **1972**, *13*, 2337–2340.
11. Mohamadi, F.; Richards, N. G. J.; Guida, W. C.; Liskamp, R.; Caufield, C.; Chang, G.; Hendrickson, T.; Still, W. C. *J. Comput. Chem.* **1990**, *11*, 440–467.
12. Weiner, S. J.; Kollman, P. A.; Nguyen, D. T.; Case, D. A. *J. Comput. Chem.* **1986**, *7*, 230–252.
13. Hasel, W.; Hendrickson, T. F.; Still, W. C. *Tetrahedron Comput. Method* **1988**, *1*, 103–116.
14. Still, W. C.; Tempczyk, A.; Hawley, R. C.; Hendrickson, T. *J. Am. Chem. Soc.* **1990**, *112*, 6127–6129.
15. Nagy, P. I.; Bitar, J.; Smith, D. A. *J. Comput. Chem.* **1994**, *15*, 1228–1240.
16. A more detailed study will be published in a more specialized journal.